Materials Chemistry and Physics 231 (2019) 335–343

Contents lists available at ScienceDirect

Materials Chemistry and Physics

journal homepage: www.elsevier.com/locate/matchemphys

Rosa damascena waste mediated synthesis of silver nanoparticles: Characteristics and application for an electrochemical sensing of hydrogen peroxide and vanillin

Totka Dodevska [a], Ivelina Vasileva [a], Petko Denev [b], Daniela Karashanova [c], Biliana Georgieva [c], Daniela Kovacheva [d], Nikoleta Yantcheva [a], Anton Slavov [a,*]

[a] Department of Organic Chemistry and Inorganic Chemistry, Technological Faculty, University of Food Technologies, 26 Maritza Blvd, Plovdiv, 4002, Bulgaria
[b] Laboratory of Biologically Active Substances, Institute of Organic Chemistry with Centre of Phytochemistry, Bulgarian Academy of Sciences, 139 Ruski Blvd, Plovdiv, 4000, Bulgaria
[c] Institute of Optical Materials and Technologies, Bulgarian Academy of Sciences, 109 Academic Georgi Bonchev Str, Sofia, 1113, Bulgaria
[d] Institute of General and Inorganic Chemistry, Bulgarian Academy of Sciences, 11 Academic Georgi Bonchev Str, Sofia, 1113, Bulgaria

ARTICLE INFO

Keywords:
Silver nanoparticles
Electrochemical sensor
Hydrogen peroxide
Vanillin
Rosa damascena waste

ABSTRACT

Silver nanoparticles (AgNPs) were synthesized by reduction of Ag^+ with four extracts of *Rosa damascena* waste: post-distillation water (PW), water extract (WE), 30% (30 EE) and 70% (70 EE) ethanol extracts. The ethanolic extracts were rich in polyphenols and particularly catechin and epicatechin (1388.01 ± 2.27 and $677.47 \pm 2.03\ \mu g mL^{-1}$, respectively) while the water extracts were rich in reducing sugars, proteins and pectic substances (for WE 254.21 ± 1.26, 296.89 ± 2.01 and $242.14 \pm 1.38\ \mu g mL^{-1}$, and for PW 185.72 ± 1.47, 298.30 ± 1.57 and $181.78 \pm 1.39\ \mu g mL^{-1}$, respectively). The morphology of AgNPs was characterized by transmission electron microscopy and the calculated average size of the AgNPs synthesized using WE and PW was 25.8 ± 11.5 nm and 11.5 ± 8.4 nm, respectively. The X-ray diffraction analysis suggested presence of silver phase which crystallized in a face centered cubic space group Fm-3m with unit cell parameter 4.085 (2) Å and mean coherent domain size 10.9 (3)nm. Biosynthesized AgNPs were deposited onto a spectroscopic graphite electrode (GE), applying two different procedures, and stabilized using chitosan to build modified electrodes-catalysts. The electrochemical performances of the modified electrodes AgNPs/GE and AgNPs/CS/GE were studied by means of cyclic voltammetry (CV), differential pulse voltammetry (DPV) and chronoamperometry at pH 7.0 and their applicability for amperometric detection of H_2O_2 and vanillin was investigated. The developed electrodes exhibited a sensitive and reproducible response for quantitative determination of H_2O_2 at applied potentials of −0.2, −0.25 and −0.3 V (vs. Ag/AgCl, 3 M KCl). Constant potential amperometry studies with AgNPs/CS/GE showed sensitive response to H_2O_2 ($115.2\ \mu A\ mM^{-1}\ cm^{-2}$) up to 6.6 mM at −0.3 V, and to vanillin ($56.8\ \mu A\ \mu M^{-1}\ cm^{-2}$) up to 0.5 mM with detection limit of 8.4 μM at 0.58 V. The results obtained from the quantitative electrochemical measurements of H_2O_2 and vanillin offer potential applications of the graphite electrodes modified with the biosynthesized AgNPs in electrochemical sensor devices for monitoring of these analytes.

1. Introduction

In the last decades, synthesis and applications of nanoparticles (NPs) with different shapes and morphologies attracts scientists, engineers and manufacturers attention. Nanomaterials based on particles with size less than 100 nm, such as, nanosheets, nanotubes, nanostrings, nanocovers, etc., possess unique and valuable properties. They have a great potential for application in medicine, for biosensors development, as catalyzers for elimination of biotoxins, for creation of electrodes with wide application in electrochemistry, for detection of substances at extremely low

* Corresponding author. 26 Maritza Blvd., Plovdiv, 4002, Bulgaria.
E-mail addresses: dodevska@mail.bg (T. Dodevska), ivelinavas@abv.bg (I. Vasileva), petkodenev@yahoo.com (P. Denev), dkarashanova@yahoo.com (D. Karashanova), biliana@iomt.bas.bg (B. Georgieva), didka@svr.igic.bas.bg (D. Kovacheva), n_iantcheva@abv.bg (N. Yantcheva), antons@uni-plovdiv.net (A. Slavov).

https://doi.org/10.1016/j.matchemphys.2019.04.030
Received 23 January 2019; Received in revised form 3 April 2019; Accepted 11 April 2019
Available online 16 April 2019
0254-0584/© 2019 Elsevier B.V. All rights reserved.

concentrations, etc. [1,2]. Despite the great number of chemical and physical methods for nanoparticles synthesis, the use of biodegradable wastes generated by agricultural and food industry is among the newest and perspective methods, based on the natural "biolaboratory". Besides, the wastes are abundant, cheap, easily available, and do not require significant pretreatment. Investigations on NPs synthesis were performed with variety of wastes: cellulose NPs from waste cotton fibers [3], silver NPs (AgNPs) using cold hardy mandarin (*Citrus unshiu*) peels [4], gold NPs employing winemaking waste [5], etc. The essential oil industry wastes are natural source of polyphenols, aroma substances, polysaccharides, proteins, etc. [6,7], compounds which are the main reducing agents of silver (and other metal cations) for NPs "green" synthesis. The lower amounts of essential oils in the raw materials (flowers, stems, leaves, etc.) results in generation of large waste quantities [8]. Although, usually the distilleries throw out the residues, these common procedures could disturb the ecological balance in the locations, and besides lead to losses of valuable biologically active substances (polyphenols, aroma substances, polysaccharides) present in the waste.

The electrochemical sensor technologies paid a special attention to the metal NPs as perspective modifiers of various kinds of electrode materials. The great surface to volume ratio, the remarkable ability to accelerate the electron transfer between electroactive substances and the electrode surface, as well as, the ability to include the nanoparticles in various configurations during development of sensor and biosensor systems are among the major reasons for the great scientific interest provoked by NPs [9–11]. A great number of scientific investigations have been focused on the development of effective electrocatalytic systems for detection of hydrogen peroxide (H_2O_2). The selective quantitative determination of H_2O_2 is extremely important due to its wide application. It has been used as oxidizer and bleaching agent in pharmaceutical, cosmetic, textile and paper industry. In food industry H_2O_2, is used for artificial aging of wines. Due to its bactericidal properties, hydrogen peroxide is used as sterilizing agent in the milk industry, as well as for ensuring packages asepticity in the brewery industry. Development of fast, reliable and cheap methods for quantitative determination of H_2O_2 is important not only for the industry but also for various biological, medical, and clinical studies because hydrogen peroxide is among the most important product of enzymatically catalyzed oxidative reactions taking place in the living organism. For this reason a lot of studies, dealing with improvement of the selectivity of H_2O_2 determination, were focused on development of effective electrocatalytical systems for H_2O_2 reduction at low potential (around and below 0 V vs. Ag/AgCl) where the interference from various substances is reduced [12]. Additionally, the development of highly effective and widely available materials with predefined electrocatalytic characteristics for quantitative determination of H_2O_2 will give an opportunity in future for construction also of first generation selective biosensors based on H_2O_2 producing oxidoreductases [13–16]. Vanillin is among the most widely used flavoring, which possesses favorable antioxidant and antimicrobial properties. Vanillin has both food and non-food applications: it is used as an additive in some foods and drinks, as a perfume fixative in various cosmetic products, in pharmaceutical preparations, etc. According to FAO, the daily intake of vanillin should be less than 10 mg kg^{-1}; in the infant food vanillin is forbidden. In this connection, the overweight content of vanillin in food products, as the excessive ingestion via the dietary intake has potential toxic effect – nausea, vomiting and headaches occurs. In the case of severe intoxication, vanillin can cause damage to human liver and kidney. Classical analytical techniques have been employed for quantitative detection of vanillin such as spectrophotometry [17], capillary electrophoresis [18] and high-performance liquid chromatography [19]. Most of these analytical methods, however, require time-consuming complex painstaking procedures for sample pre-treatment, as well as expensive and sophisticated instruments. Therefore, the importance of improved analytical methods for determination of vanillin has received considerable attention. Vanillin is an electroactive and can be quantified electrochemically. In comparison with the aforementioned techniques, electrochemical analysis has been considered as a low-cost and effective way due to its intrinsic simplicity and selectivity. The electrochemical sensing systems are a promising alternative of the traditional analytical techniques, since they provide opportunity for an accurate, highly sensitive and susceptible to automatization analysis. Therefore, the development of novel electrochemical sensors has been a topic of research nowadays [20–23].

The AgNPs are among the most synthesized metal NPs due to their valuable properties and various applications: efficient antibacterial activities [24], anti-larvicidal activity [25], catalytic activities for pollutants removal [26], obtaining of biosensors [27], etc. The present study focuses on the utilization of the rose oil industry waste for "green" synthesis of AgNPs and their application for development of modified electrodes for amperometric sensing of H_2O_2 and vanillin. Additionally, it investigates the influence of extracts composition and type of the extractant on the process of NPs synthesis.

2. Materials and methods

2.1. Materials

The waste materials (obtained after hydrodistillation of Bio certified *Rosa damascena* Mill) were obtained from ECOMAAT distillery (Mirkovo, Bulgaria – 2016 harvest).

All the reagents used: $Na_2HPO_4.12H_2O$, $NaH_2PO_4.2H_2O$ and vanillin (4-Hydroxy-3-methoxybenzaldehyde) (Sigma-Aldrich, Germany); $AgNO_3$, NaOH, CH_3COOH (Merck, Germany); 95% ethanol, H_2O_2 (Fluka, Germany); chitosan (Acros, Belgium) were of analytical grade and obtained from local distributors. The standard compounds (D-glucose, galacturonic acid, gallic acid, 3,4-dihydroxy benzoic acid, chlorogenic acid, caffeic acid, *p*-coumaric acid, ferulic acid, ellagic acid, catechin, epicatechin, rutin, naringin, myricetin, quercetin, naringenin and kaempferol) were purchased from Sigma-Aldrich (Steinheim, Germany). Phosphate buffer solution PBS (0.1 M; pH 7.0) was prepared by dissolving appropriate amounts of $Na_2HPO_4.12H_2O$ and $NaH_2PO_4.2H_2O$ in double distilled water. The pH was adjusted by adding 0.1 M NaOH.

2.2. Methods

2.2.1. Preparative methods

2.2.1.1. Preparation of post-distillation water and extracts from Rosa damascena waste. After the end of essential oil distillation, the residual mass was removed from the still by screw conveyor and pressed to separate both phases. The liquid phase (post-distillation water, PW) obtained was collected, filtered and further used for AgNPs synthesis. The remaining solid waste materials were dried at 50 °C under vacuum and were used for obtaining of water and water-ethanolic extracts as follow: 7.5 g of dried *Rosa damascena* wastes were treated at 25 °C for 24 h at constant stirring with water, 30 and 70% ethanol (50 mL). Then the mass was filtered and the obtained extracts were denoted water extract (WE), 30% ethanol extract (30 EE) and 70% ethanol extract (70 EE) – obtained with extractants water, 30% and 70% ethanol, respectively.

2.2.1.2. "Green" synthesis of AgNPs. Silver nanoparticles were synthesized with post-distillation water (PW) and three water/water-ethanolic extracts of *Rosa damascena* waste by mixing 1 mL (extract or post-distillation water), 3 mL 0.01 M $AgNO_3$ and 1 mL double distilled water.

2.2.1.3. Assembling of AgNPs modified graphite electrode. The spectroscopic graphite electrode (RWO, Ringsdorf, Germany; geometrical surface area 25 mm^2) was prepared for modification by mechanical

polishing with emery paper (P800, P1200 and P2000), rinsed and sonicated in with double distilled water for 5 min. The working surface of the cleaned and polished graphite electrode (GE) was modified using two different approaches:

1). Under static conditions by immersing the graphite electrode in the colloidal AgNPs solution; the duration of the adsorption process was 2 h at temperature 25 °C. The modified electrode will be further denoted as electrode type AgNPs/GE;
2). Through a dropwise addition of 40 μL of the colloidal AgNPs solution. After applying the electroactive substance, the electrode surface was dried at room temperature. In order to stabilize the electroactive layer, a thin polymer film was applied by dropping onto the electrode surface of 5 μL 0.5% chitosan (in a solvent 0.1 M CH_3COOH) and drying it in air. The resulting modified electrode will be denoted as electrode type AgNPs/CS/GE.

2.2.2. Analytical methods

2.2.2.1. Determination of extracts composition. The dry matter content in the extracts was determined with Kern MLB 50-3 moisture analyzer (Kern & Sohn GmbH, Germany).

The reducing sugars in the extracts were determined by the PAHBAH method [28] with slight modifications. Briefly, 750 μL of PAHBAH (4-hydroxybenzoic acid hydrazide; Sigma-Aldrich, Germany) reagent was added to 250 μL properly diluted polysaccharide solution. The mixture was boiled for 5 min in a water bath and then cooled (5 min) in an ice bath. The absorbance was measured at 410 nm against blank prepared with distilled H_2O. The standard curve was prepared with D-glucose solutions in the 5–100 μg mL^{-1} concentration range.

The uronic acid content of the extracts was determined by the *m*-hydroxybiphenyl method [29] using galacturonic acid as standard. The total carbohydrate content was measured by the phenol-sulfuric acid method [30] using D-glucose as standard. The protein content was assessed by the Bradford method [31] using AMRESCO E535-KIT (AMRESCO, Solon, Ohio, USA), and bovine gammaglobulin as standard.

Individual phenolic compounds in the extracts were determined on an Agilent 1220 HPLC system (Agilent Technology, USA) as described by Slavov et al. [7]. The polar volatile and non-volatile substances in the extracts were determined by GC-MS using Agilent GC 7890 with mas-selective detector Agilent MD 5975 and column HP-5ms [32]. The individual compounds were identified comparing the retention times and the relative index (RI) with those of standard substances and mas-spectral data from libraries of The Golm Metabolome Database (http://csbdb.mpimp-golm.mpg.de/csbdb/gmd/gmd.html) and NIST′08 (National Institute of Standards and Technology, USA).

2.2.2.2. UV–vis spectroscopy measurements. UV–Vis measurements of the AgNPs synthesis was carried out on a Helios Omega spectrophotometer (Thermo Scientific, Madison, WI, USA) equipped with VISIONlite software and operated at a resolution of 1 nm. The scanning was performed in the 350–700 nm range at scan speed 1600 nm min^{-1}.

2.2.2.3. Infrared spectroscopy measurements. The infrared (IR) spectra of the investigated pectic polysaccharides were taken using a Nicolet iS10 (Thermo Fisher Scientific, USA) spectrometer with ATR Thermo Scientific Smart Orbit and active sample surface of 1.5 mm^2. The extracts and the AgNPs were lyophilized and the lyophilizates were analyzed in the 4000-400 cm^{-1} range at a 4 cm^{-1} resolution. Each spectrum was recorded after 128 scans. The spectra were analyzed using Spekwin32 software.

2.2.2.4. Transmission electron microscopy (TEM) of AgNPs. The samples of the green synthesized AgNPs were prepared for TEM analysis by placing a drop of the suspension on a standard copper grid, covered by amorphous carbon layer and allowing the water to evaporate at room temperature. Observations and micrographs were acquired with high resolution transmission electron microscope JEOL JEM 2100 (JEOL, Japan) at accelerating voltage 200 kV in conventional and high resolution modes for TEM and HRTEM images, respectively. Statistical analysis of AgNPs particles size distribution was carried out with Image J software [33]. The identification of the phase composition of the samples was achieved using PDF-2 Database of the International Center for Diffraction Data (ICDD).

2.2.2.5. X-ray diffraction analysis of AgNPs. Powder X-ray diffraction patterns were collected within the range from 5.3 to 80° 2θ with a constant step 0.02° 2θ on Bruker D8 Advance diffractometer with Cu Kα radiation and LynxEye detector. Phase identification was performed with the Diffrac*plus* EVA using the same Database as for TEM diffraction patterns indexing. Unit cell parameters and mean crystallite size were determined with the Topas-4.2 software package using the fundamental parameters peak shape description including appropriate corrections for the instrumental broadening and diffractometer geometry.

2.2.2.6. Electrochemical measurements. All the electrochemical measurements were performed using potentiostat EmStat3 (PalmSens BV, The Netherlands) interfaced with a computer and controlled by PSTrace 5.5 software. A conventional thermostated three-electrode cell including a working electrode (the bare GE or GE modified with AgNPs), an Ag/AgCl (3 M KCl) as a reference electrode (Hanna Instruments S.R.L., Romania), and a platinum wire as a counter electrode was used. The modified electrode was investigated using cyclic voltammetry (CV), differential pulse voltammetry (DPV) and chronoamperometry at a constant potential. All the electrochemical experiments were carried out at 25 °C in 0.1 M PBS purged with argon. The DPV parameters were chosen as follows: scan rate 9 mV s^{-1}, pulse amplitude 50 mV, pulse interval 70 ms. The experimental data were processed by software package "OriginPro 8".

2.3. Statistical analysis

The analyses were run three times and the data are given as mean values. Statistical significance was detected by analysis of variance (ANOVA, Tukey's test; value of $p < 0.05$ indicated statistical difference).

3. Results and discussion

3.1. "Green" synthesis of silver nanoparticles and UV–Vis studies

The formation of AgNPs started almost immediately after mixing the WE and $AgNO_3$ solution, and around the 5th minute the color of the solution turned to light brown which could be attributed to synthesis of AgNPs. The solution was already dark brown at the 15th minute (Supplementary Material 1).

The other extracts gave AgNPs with significant delay in time: the PW started to induce AgNPs formation at around the 30^{th} min and at the 60^{th} min the color of the solution was dark brown. The 30 EE and 70 EE gave AgNPs at around the 120^{th} and the 360^{th} minutes, respectively.

The results of visual observations of AgNPs "green" synthesis were also confirmed by the UV–Vis spectrophotometry measurements.

The intensive absorption was observed after the 45th minute of mixing $AgNO_3$ and WE (Supplementary Material 2A). In fact, after the 60^{th} minute the absorbance values became unreadable due to the intensive AgNPs formation and probably agglomeration to a certain extent of the nanoparticles. The absorption of PW synthesized AgNPs became more intensive after the 45th minute and at the 60^{th} minute (visually also around the 60^{th} minute was observed darkening of the solution) implied clearly the nanoparticles formation (Supplementary Material 2B). Both ethanolic extracts were able to induce AgNPs

synthesis, although with significant delay: at the 120th minute and the 360th minute for 30 EE and 70 EE, respectively (Supplementary Material 2C and 2D).

3.2. Characteristics of the extracts and the post-distillation water

The preliminary results for AgNPs synthesis suggested that the type of the extractant and the composition of the extracts influenced significantly the formation of AgNPs which could be important for the AgNPs further applications. The pH of all the extracts was adjusted to 5.5 in order to eliminate the influence on the AgNPs synthesis. In most of the studies possibilities for synthesis of NPs with different plant extracts were reported [4,27,34] but the extracts were not chemically investigated or the characterization was perfunctory. Besides, no comparison on the influence of the type of the extractant and the extracted substances on the synthesis and application of NPs was made. For this reason in the subsequent experiments the extracts and the PW were investigated for their chemical composition (Table 1).

The previous studies for metal NPs synthesis suggested [27] that polyphenols were among the main compounds responsible for nanoparticle synthesis. Based on these conclusions in the subsequent experiments the extracts were investigated for individual polyphenol substances (Table 1). Confronting the data it could be suggested that the ethanolic extracts had higher content of phenolic acids and flavonoids than water extracts. Catechin and epicatechin had the highest concentrations in 70 EE: 1388.01 ± 2.27 and 677.47 ± 2.03 μg mL^{-1}, respectively. On the other hand, the water extracts were rich in carbohydrates (including reducing sugars), proteins and pectic substances (as suggested by the presence of uronic acids). Some studies suggested that the biomacromolecules present in plant extracts (predominantly in water extracts) play a dual role in the NPs synthesis: as a reducing agent, and furthermore for capping and stabilization of metal NPs [35].

Industrially steam distillation of essential oil crops never leads to complete extraction of the aroma substances [6,7]. This is mainly due to economic reasons (the technological time necessary to distill most of the aroma substances) and retention of the substances in the plant matrix. This observation suggests that the essential oil industry wastes have a potential for extraction of residual volatile polar metabolites. Besides, the waste is rich in non-volatile polar metabolites (flavonoids, organic acids, carbohydrates, amino acids, etc.) and some of these compounds have also reduction properties and could influence the synthesis and stabilization of AgNPs [27]. For this reason in the subsequent experiments, the individual polar volatile and non-volatile substances present in the extracts were determined by GC-MS (Supplementary material 3 and 4).

The results from the analyses for polar volatile and non-volatile substances in the extracts suggested that the waste was rich source of β-phenethyl alcohol, geraniol, β-citronellol and some hydrocarbons. Monosaccharides, such as fructose, glucose and galactose were prevalent in water extracts while gallic acid, caffeic acid and amino acids were equally found in all extracts.

3.3. Infrared spectroscopy studies of the extracts before and after AgNPs synthesis

The infrared spectroscopy studies were performed in order to obtain information about the functional groups of the compounds in the extracts involved in the "green" synthesis of AgNPs. A number of bands were identified in the spectra (Supplementary material 5) and they could be assigned as follow: around 3340 cm^{-1} due to the absorption of the hydroxyl groups; around 1340-1330 cm^{-1} due to the phenolic OH group and hydroxyl groups of the pyranose ring of the carbohydrate moieties. According to some studies, the phenolic compounds were among the main contributors to the bio-reduction process [27] and the shifts in the bands of the IR spectra of the extracts and the bio-synthesized AgNPs confirmed this suggestion. The bands at 1730 cm^{-1} in WE could be assigned as the C—O and C═O stretching modes of the carbonyl functional group in ketones, aldehydes and carboxylic acids. Around 1630-1640 cm^{-1} were observed bands characteristic for amide linkage and their shifts could suggest the involvement of proteins in the process of synthesis and capping of AgNPs [36]. The bands around 820 cm^{-1} and their shifts are due rocking vibrations of NH groups and suggested involvement of proteins in the process. Proteins bind well and have strong affinity to AgNPs and this increases the stabilization of the nanoparticles [37,38].

Table 1
Composition of extracts of *Rosa damascena* waste.

Parameter	WE	PW	30 EE	70 EE
Dry matters (DM), %	2.24 ± 0.20^{a}	2.36 ± 0.17^{a}	3.45 ± 0.18^{b}	3.68 ± 0.21^{b}
Reducing sugars, μg mL^{-1}	254.21 ± 1.26^{a}	185.72 ± 1.47^{b}	150.40 ± 1.68^{c}	98.26 ± 1.47^{d}
Uronic acid content, μg mL^{-1}	242.14 ± 1.38^{a}	181.78 ± 1.39^{b}	58.06 ± 1.95^{c}	37.67 ± 1.54^{d}
Neutral sugars, μg mL^{-1}	353.35 ± 1.66^{a}	386.62 ± 2.11^{b}	211.48 ± 1.84^{c}	184.25 ± 1.36^{d}
Proteins, μg mL^{-1}	296.89 ± 2.01^{a}	298.30 ± 1.57^{a}	82.37 ± 1.65^{b}	18.14 ± 1.88^{c}
Phenolic acids, μg mL^{-1}				
Chlorogenic acid	7.68 ± 0.85^{a}	15.48 ± 0.96^{b}	63.61 ± 1.41^{c}	79.43 ± 1.13^{d}
Neochlorogenic acid	70.11 ± 1.25^{a}	80.53 ± 1.95^{b}	140.70 ± 2.14^{c}	162.03 ± 1.95^{d}
Caffeic acid	9.34 ± 0.36^{a}	19.17 ± 0.97^{b}	51.10 ± 1.10^{c}	72.38 ± 1.41^{d}
p-Coumaric acid	4.12 ± 0.24^{a}	11.83 ± 0.68^{b}	33.09 ± 0.87^{c}	40.33 ± 1.20^{d}
Ferulic acid	4.83 ± 0.67^{a}	6.08 ± 1.01^{a}	41.47 ± 1.16^{c}	107.22 ± 1.62^{d}
Ellagic acid	2.86 ± 0.12^{a}	8.65 ± 0.64^{b}	54.60 ± 0.95^{c}	125.84 ± 1.46^{d}
3,4-dihydroxy-benzoic acid	39.11 ± 1.65^{a}	35.88 ± 1.84^{a}	76.74 ± 1.23^{c}	143.13 ± 1.91^{d}
Flavonoids, μg mL^{-1}				
Quercetin	18.12 ± 1.01^{a}	33.31 ± 1.99^{b}	225.27 ± 2.30^{c}	305.15 ± 2.55^{d}
Quercetin-3-β-glucoside	36.46 ± 2.86^{a}	74.25 ± 1.93^{b}	239.87 ± 2.04^{c}	285.04 ± 1.81^{d}
Myricetin	8.75 ± 0.95^{a}	9.57 ± 1.02^{a}	56.01 ± 1.33^{c}	110.62 ± 1.43^{d}
Kaempferol	1.52 ± 0.23^{a}	2.70 ± 0.35^{a}	4.40 ± 0.47^{c}	19.31 ± 0.68^{d}
Naringin	48.62 ± 1.27^{a}	108.66 ± 1.26^{b}	207.41 ± 1.59^{c}	375.57 ± 1.89^{d}
Catechin	142.33 ± 2.16^{a}	262.70 ± 2.36^{b}	992.24 ± 2.58^{c}	1388.01 ± 2.27^{d}
Epicatechin	43.38 ± 0.89^{a}	71.47 ± 1.52^{b}	450.46 ± 1.98^{c}	677.47 ± 2.03^{d}

WE – water extract.
PW – post-distillation water.
30 EE – 30% ethanolic extract.
70 EE – 70% ethanolic extract.
$^{a, b, c, d}$ - Different letters in a row mean statistical difference (Tuckey's HSD test, $p < 0.05$).

3.4. TEM analyses and characterization of AgNPs

Furthermore, the AgNPs were examined by TEM. Having in mind the preliminary results for synthesis of AgNPs and the UV–Vis studies (Supplementary materials 1 and 2) only silver nanoparticles obtained with WE and PW were investigated. The TEM analysis clearly demonstrated the formation of nanoparticles in both cases, presented in (Fig. 1A and B), respectively. They were silver metal crystalline, as it was unambiguously proved by indexation of selected area electron diffraction (SAED) patterns (Fig. 1C and D) and by measured HRTEM interplanar distances. The TEM micrographs (Fig. 1A and B), visualizing AgNPs nanoparticles with larger diameters (30–50 nm) implied that their shapes could be described as irregular. From the studies carried out on the metal NPs with plant extracts it can be concluded that if the phytochemical composition was rich on polyphenols, flavonoids, tannins, carbohydrates and phenolic acids, there is a high probability of achieving spherical nanoparticles [39]. This conclusion was confirmed by the results in the present study only for small sized AgNPs (Fig. 1 HRTEMs), due to inevitable aggregation of the particles after the synthesis process and visualization of the crystalline aggregates with irregular shapes and sizes over 30 nm. Size distribution histograms of the particles and the mean particle size were determined (Fig. 1E and F). The average size of the AgNPs synthesized with WE and PW were calculated to be 25.8 ± 11.5 nm and 11.5 ± 8.4 nm, respectively. The average size of the AgNPs synthesized was much smaller than the obtained by Parameshwaran et al. [40] (73.2 and 82.8 nm, in alkaline and acidic medium, respectively) and Phatak et al. [37] (84.85 nm), and was comparable with the size of the AgNPs (around 25 nm) synthesized by Kumar et al. [24] and Roopan et al. [25]. In a recent study Pinto et al. [41] investigated the relation between the concentration of phenolic compounds of a plant extract and the size of the NPs synthesized and found that the higher the concentration the smaller the nanoparticles size. Confronting the results from histograms (Fig. 1E and F) with the data of individual polyphenolic compounds content (Table 1) it could be confirmed that the higher the concentrations of polyphenols in the extract the smaller is the average NPs size. Besides, from visual observation experiments and UV–Vis studies could be concluded that the faster the process of AgNPs synthesis the higher the nanoparticles agglomeration with time.

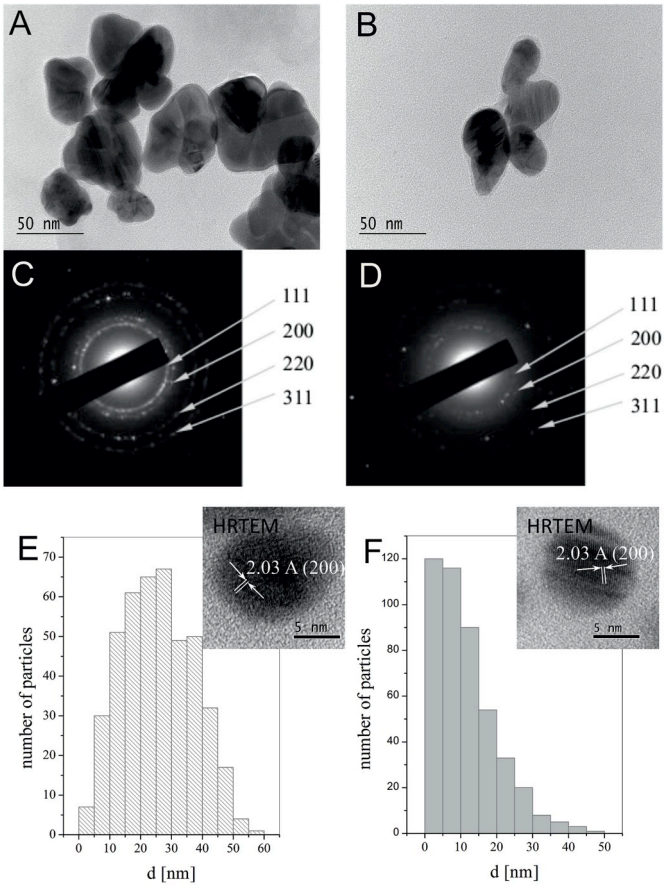


Fig. 1. TEM micrographs, SAED patterns, histograms of the size distribution of AgNPs and HRTEM micrographs as insets, obtained with WE are presented on (A), (C) and (E) and for AgNPs synthesized with PW on (B), (D) and (F), respectively. SAED patterns and HRTEM micrographs are indexed according to PDF 87–0720 for cubic Ag.

3.5. X-ray diffraction analysis of AgNPs

In the subsequent experiments, the NPs synthesized with WE and PW were subjected to X-ray diffraction (XRD) analysis which confirmed the AgNPs synthesis and the TEM results. Mixture of sample WE and $AgNO_3$ was found to contain silver (Ag) phase which crystallize in a face centered cubic space group Fm-3m with unit cell parameter a = 4.085 (2)Å and mean coherent domain size 10.9 (3) nm. Similar observations were made by Velusamy et al. [42] and Parameshwaran et al. [40] investigating AgNPs synthesized using aqueous solutions of neem gum and *Beta vulgaris*, respectively. An additional amorphous phase is presented in the sample with two humps at around 5.46 Å and 2.98 Å. The AgNPs synthesized with PW also was found to contain silver (Ag) phase which crystallize in a face centered cubic space group Fm-3m with unit cell parameter a = 4.085 (2)Å and mean coherent domain size 13.2 (5) nm (Supplementary Material 6).

3.6. Electrocatalytic activity of the AgNPs in reduction of H_2O_2

The electrocatalytic behavior of AgNPs was further studied using cyclic voltammetry (CV) and chronoamperometry. Fig. 2A presents cyclic voltammograms (CV) of the modified electrode type AgNPs/GE and the bare graphite electrode in 0.1 M PBS (pH 7.0) recorded in the potential range from −0.2–0.8 V at scan rate of 25 mV s^{-1}. No peaks were observed in the scan range on the bare graphite electrode (inset). In comparison, a pair of well-defined redox peaks was observed at 0.1 V and 0.5 V, respectively, which could be attributed to the Ag(I)/Ag (0) redox couple, demonstrating the existence of AgNPs on the surface of graphite electrode. The CV of the same electrode recorded at scan rate of 10 mV s^{-1} confirms that the values of Ep^a and Ep^c shift slightly to the positive and negative directions, respectively, and ΔEp increases with increasing the scan rate.

The electrocatalytic activity of the AgNPs/GE was further investigated in the presence of 3 mM H_2O_2 in deaerated 0.1 M PBS (Fig. 2B). Upon addition of H_2O_2 into the solution, an obvious cathodic current increment was observed for the modified electrode, which can be attributed to the catalytic process of H_2O_2 reduction. The peak potential appeared at −0.4 V and shifted positively compared with that of silver particles modified electrodes previously reported [43,44], indicating that the electrode modified with biosynthesized AgNPs, exhibited excellent electrocatalytic activity towards H_2O_2.

In the next step, the graphite electrodes modified with AgNPs (type AgNPs/GE and type AgNPs/CS/GE) were tested for amperometric quantitative detection of H_2O_2. The concentration dependence of the amperometric response of the electrodes was investigated by means of constant potential amperometry at potentials of −0.3, −0.25 and −0.2 V. Fig. 2C displays the current response of the modified electrode AgNPs/CS/GE upon successive addition of H_2O_2 into the stirring 0.1 M PBS (pH 7.0) at an applied potential of −0.2 V. A well-defined stepwise increasing cathodic current was observed during the successive additions of 0.5 mM H_2O_2. The chronoamperometric record indicated that the reductive current increased stepwise upon introducing in the buffer aliquots of the H_2O_2 stock solution. These results evidenced a stable and

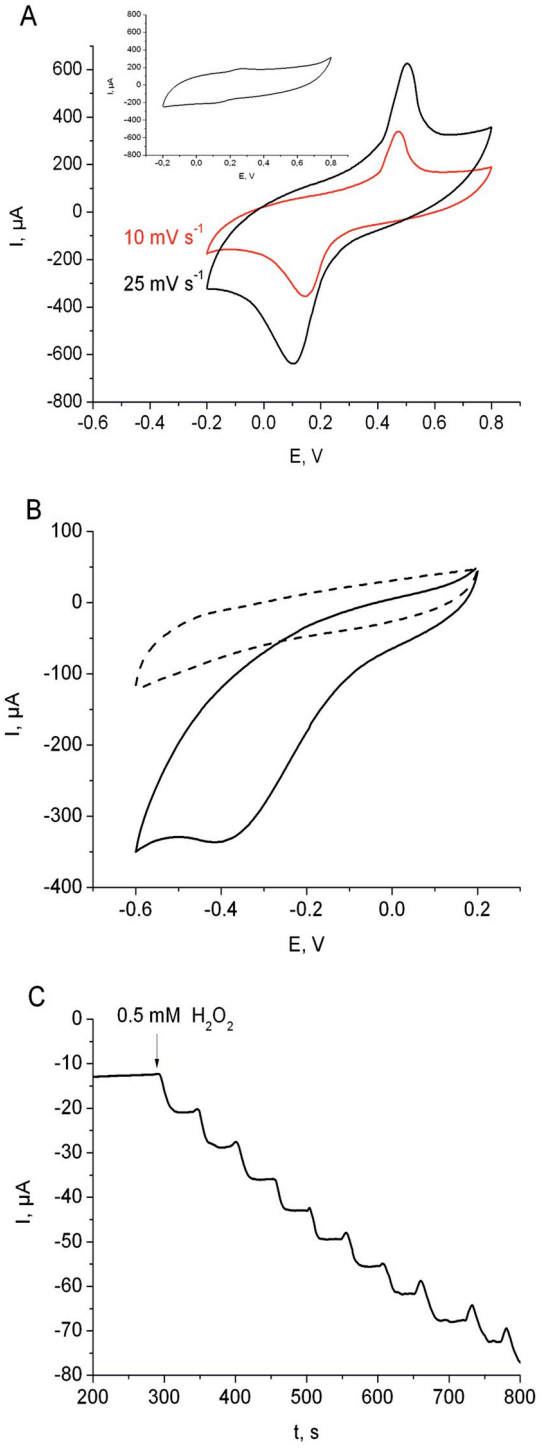


Fig. 2. Characteristics of the AgNPs modified graphite electrodes: (A). Cyclic voltammorgams (CVs) of the modified electrode AgNPs/GE in 0.1 M PBS (pH 7.0) at scan rates of 10 and 25 mV s^{-1}. Inset: CV of the bare graphite electrode (GE); (B). Cyclic voltammorgams of GE (dash line) and AgNPs/GE (solid line) electrodes in the presence of 3 mM H_2O_2 in 0.1 M PBS (pH 7.0); scan rate: 50 mV s^{-1}; (C). Amperometric response of AgNPs/CS/GE to successive addition of 0.5 mM H_2O_2 into stirring 0.1 M PBS (pH 7.0); applied potential: −0.2 V.

efficient catalytic property of the biosynthesized AgNPs. As shown, immediately after the injection of H_2O_2, AgNPs/CS/GE responded rapidly to the changes of H_2O_2 concentration, producing steady-state signal within 10 s.

The calibration plots (Fig. 3) for the both modified electrodes showed

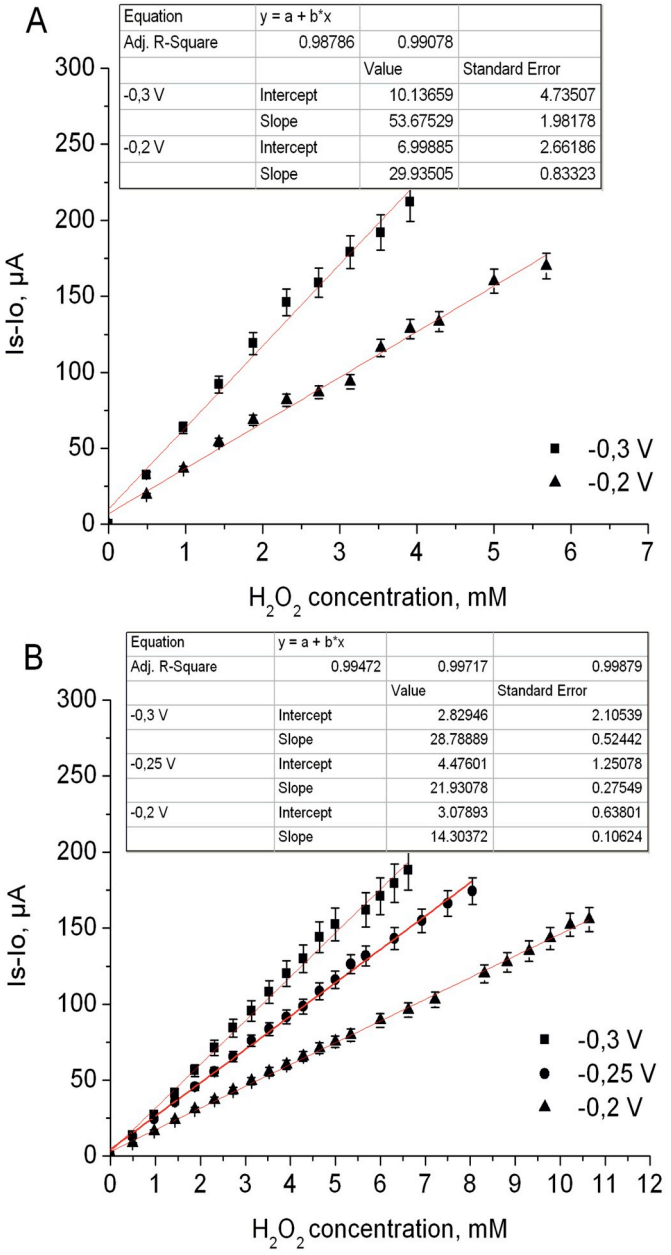


Fig. 3. Background corrected steady-state response of the modified electrodes AgNPs/GE (A). and AgNPs/CS/GE (B). as a function of H_2O_2 concentration; supporting electrolyte: 0.1 M PBS (pH 7.0).

that the sensitivity increased and the range of the linear concentration dependence of the signal shortened as the applied potential shifts to the negative direction. As a general rule, the electrode sensitivity at potential of −0.3 V was found to be about twice as high as the sensitivity registered at −0.2 V.

Based on the calibration plot, the sensitivity of the modified electrode type AgNPs/GE in the detection of H_2O_2 at potential of −0.3 V was found as 53.7 μA mM^{-1}. Calculated specific electrode sensitivity (214.7 μA mM^{-1} cm^{-2}) is about 18 times as high as the one achieved by Zhang et al. [43] by means of Ag–HNTs–MnO_2 composite-based modified electrode.

Table 2 represents an overview on the main operational parameters of the electrodes modified with biosynthesized AgNPs. The sensitivity of the electrode type AgNPs/GE was found to be 2 times higher than this one of AgNPs/CS/GE estimated under the same conditions. The experimental data indicated that the range of the strict linear dependence of

Table 2
Operational parameters of graphite electrodes modified with biosynthesized AgNPs; reference electrode Ag/AgCl, 3 M KCl; background electrolyte 0.1 M PBS (pH 7.0).

Type of modified electrode	Applied potential, V	Electrode sensitivity, μA $mM^{-1}cm^{-2}$[a]	r^2	Linearity[b], mM
AgNPs/GE	−0.3	214.7	0.98_9	3.9
	−0.2	119.7	0.99_1	5.6
AgNPs/CS/GE	−0.3	115.2	0.99_5	6.6
	−0.25	87.7	0.99_7	8.0
	−0.2	57.2	0.99_9	10.6

[a] The electrode sensitivity was determined as the slope of the linear portion of the calibration graph divided by geometric electrode area.
[b] The linear portion of the calibration graph.

the electrode signal for AgNPs/CS/GE was significantly longer as compared with this parameter resolved for electrode AgNPs/GE under the same working potential. This extension in the linearity of the current response, observed for the modified electrode type AgNPs/CS/GE, evidenced the stabilizing effect of the chitosan coating deposited onto the modified graphite surface.

Detection and fabrication reproducibility of the modified electrode AgNPs/CS/GE also were examined. To characterize the reproducibility, five independent repetitive measurements were performed in presence of 1 mM H_2O_2 by constant potential amperometry at −0.3 V and −0.2 V using the same modified electrode. At an applied potential of −0.3 V in the presence of 1.0 mM H_2O_2 the electrode response was 27 ± 1.8 μA and the relative standard deviation (R.S.D.) was calculated to be 6.7%. Analogous studies carried out at potential of −0.2 V show electrode response of 16.4 ± 0.9 μA and R.S.D. of 5.5%. The results prove that the modified electrode possesses satisfactory reproducibility of the current signal. The fabrication reproducibility of three independently made electrodes also showed an acceptable reproducibility – R.S.D. of 9.3% (evaluated at −0.2 V by current signal to 1 mM H_2O_2).

The analytical behavior of the developed modified electrodes can be appreciated by comparative study with other amperometric electrodes for H_2O_2 detection based on Ag particles. We have summarized various H_2O_2 sensors in Table 3 with respect to the applied potential, the sensitivity and the linearity of detection in neutral medium. From the data presented it can be seen that the operational characteristics of the modified with biosynthesized AgNPs electrodes are in general comparable with other electrodes modified with electrochemically deposited Ag particles. It should be noted that the operational parameters of the here proposed electrodes are superior in some cases, especially in sensitivity and working potential. In contrast to other H_2O_2 amperometric sensors based on Ag particles of previous literature reports [44–48,50], the applied potential for the here reported modified electrodes is less negative. At low potentials the background current decreases and the response of other electroactive species can be minimized or totally eliminated, which is crucial for the selectivity of the analytical system.

3.7. Application of AgNPs modified electrode for vanillin sensing

The performance of the modified electrode AgNPs/CS/GE regarding the sensing of vanillin was evaluated using two electrochemical techniques – DPV and constant potential amperometry, according to the sensitivity, linear range and detection limit. Fig. 4A presents the DPV curves of vanillin with different concentrations. The peak current was proportional to the vanillin concentration and it can be expressed in a model such as: $y = ax + b$, where a is the slope of the calibration curve in terms of sensitivity. The linear regression equation was as follows: I_p (μA) = 0.03519C (μM) + 7.3743 and was accomplished with a correlation coefficient of 0.989 (Fig. 4A, inset). The proposed electrode exhibited electrochemical sensitivity of 140.76 μA μM^{-1} cm^{-2} (normalized to the electrode geometric surface area) up to 1.1 mM vanillin.

The amperometric response for the modified electrode was evaluated with successive additions of vanillin at a fixed potential. Fig. 4B displays the authentic record of the amperometric response of electrode to successive additions (in 60 s intervals) of vanillin stock solution at a constant applied potential of 0.58 V under constant stirring. Upon addition of vanillin the modified electrode shows increasing staircase current response, corresponding to the electrochemical oxidation of the analyte. Steady-state current value was reached within 20 s. The background subtracted steady-state response of the electrode (Fig. 4B, inset) was proportional to the vanillin concentration up to 500 μM (correlation coefficient of 0.976) with sensitivity of 56.8 μA μM^{-1} cm^{-2}. The limit of detection was 8.4 μM, defined at a signal-to-noise ratio of 3.

The linear dynamic range of the analysis reported in the present work was wider than most of the reported previously [20–23]. Although the limit of detection of vanillin with the here presented electrode is higher, this method for surface modification has made significant progress in electrode preparation, in terms of simplicity, reduced cost and eco-friendly methodology.

4. Conclusions

The present work demonstrated for the first time utilization of *Rosa damascena* waste for synthesis of AgNPs and applicability of the nanoparticles for development of sensors for hydrogen peroxide and vanillin detection. The process of AgNPs synthesis takes place in one-stage and is based on utilization of abundant and cheap waste materials. Besides, it is potential approach for utilization of rose oil industry waste. The extracts

Table 3
Comparison of the operational characteristics of modified with AgNPs electrodes for H_2O_2 amperometric detection reported in the literature with the achieved in the present work.

Electrode modifier/(Electrode)	Applied potential, V	Supporting electrolyte	Sensitivity, μA mM^{-1} cm^{-2}	Linearity, mM	Reference
Ag–HNTs–MnO_2/(GC)	−0.3[b]	0.1 M PBS, pH 7.2	11.9	4.71	[43]
Ag micro-spheres/(GC)	−0.5[b]	0.2 M PBS, pH 7.0	180.6[c]	2	[44]
Ag microparticles/(SPC)	−0.4[a]	0.01 M PBS, pH 7.4	138.4	14.2	[45]
AgNPs/ZnO NRs/(FTO)	−0.55[a]	0.1 M PBS, pH 7.0	152.1	0.983	[46]
AgNPs/PANI/HNTs/(GC)	−0.2[b]	0.1 M PBS, pH 7.0	74.8	4.7	[47]
Ag dendrite/(GC)	−0.2[a]	0.1 M PBS, pH 7.6	104.53	12	[48]
Graphene-AgNPLs/(GC)	−0.5[a]	0.2 M PBS, pH 7.0	183.5	10	[49]
PVA-Ag/(Pt)	−0.5[b]	PBS, pH 7.0	4090	1.0	[50]
Ag-Nafion/(CF microelectrode)	0[a]	Britton-Robinson buffer, pH 7.0	–	100	[51]
AgNPs/GE	−0.3[a]	0.1 M PBS, pH 7.0	214.7	3.9	Present work
AgNPs/CS/GE			115.2	6.6	

[a] Referred to an Ag/AgCl (3 M KCl) electrode (0.200 V vs. SHE).
[b] Referred to a saturated calomel electrode (SCE) (0.242 V vs. SHE).
[c] The sensitivity was estimated from the data in the paper.

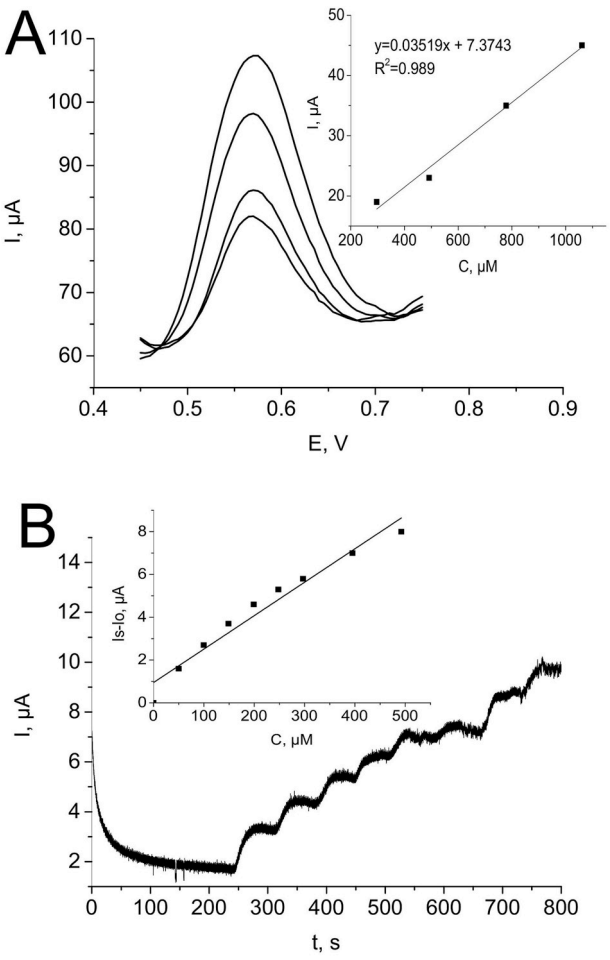


Fig. 4. A. DPVs of the modified electrode AgNPs/CS/GE in the presence of various concentrations of vanillin in PBS (pH 7.0). Inset: linear relationship between the peak current and the concentration; B. Amperometric response of AgNPs/CS/GE in PBS (pH 7.0) for successive additions (6 injections of 50 μM and 2 injection of 100 μM vanillin) at potential of 0.58 V. Inset: the corresponding calibration plot.

(PW, WE, 30 EE and 70 EE) were rich in various substances, such as phenolic acids, flavonoids, proteins, terpenes, carbohydrates, etc. having important role in reduction of Ag^{+} and NPs formation. The main functional groups involved in the synthesis were aromatic hydroxyl groups and carbonyl groups. Furthermore, proteins, polysaccharides and carboxylic acids additionally participated in the process by capping the *in situ* generated nanoparticles. The TEM micrographs suggested that nanoparticles were obtained as sphere-like particles with average size of the AgNPs synthesized with WE and PW calculated to be 25.8 ± 11.5 nm and 11.5 ± 8.4 nm, respectively. The biosynthesized AgNPs were used for assembling of working electrode for H_2O_2 and vanillin sensing. The developed electrodes exhibited a sensitive and reproducible response for quantitative determination of H_2O_2 at applied potentials of −0.2, −0.25 and −0.3 V (vs. Ag/AgCl, 3 M KCl). Constant potential amperometry studies with AgNPs/CS/GE showed sensitive response to H_2O_2 (115.2 μA mM^{-1} cm^{-2}) up to 6.6 mM at −0.3 V, and to vanillin (56.8 μA μM^{-1} cm^{-2}) up to 0.5 mM with detection limit of 8.4 μM at 0.58 V. Nevertheless, the catalytic activity of the proposed electrode in both target reactions (reduction of H_2O_2 and oxidation of vanillin), in terms of sensitivity and limit of detection, could be improved by optimizing the amount of AgNPs suspension, applied for modification of the graphite carrier, as well as the type of the used protective layer.

Conflicts of interest

Declarations of interest: none.

Acknowledgement

We acknowledge the financial support from the National Science Fund of Bulgaria; project DN 17/22 “Valorization and application of essential oil industry wastes for “green” synthesis of metal nanoparticles”.

Appendix A. Supplementary data

Supplementary data to this article can be found online at https://doi.org/10.1016/j.matchemphys.2019.04.030.

References

[1] H. Fu, X. Yang, X. Jiang, A. Yu, Bimetallic Ag-Au nanowires: synthesis, growth mechanism, and catalytic properties, Langmuir 29 (2013) 7134–7142. https://doi.org/10.1021/la400753q.

[2] Y. Xia, H. Yang, C.T. Campbell, Nanoparticles for catalysis, Acc. Chem. Res. 46 (2013) 1671–1672. https://doi.org/10.1021/ar400148q.

[3] T.F. Meyabadi, F. Dadashian, G.M.M. Sadeghi, H.E.Z. Asl, Spherical cellulose nanoparticles preparation from waste cotton using a green method, Powder Technol. 261 (2014) 232–240. https://doi.org/10.1016/j.powtec.2014.04.039.

[4] N. Basavegowda, Y. Rok Lee, Synthesis of silver nanoparticles using Satsuma Mandarin (*Citrus unshiu*) peel extract: a novel approach towards waste utilization, Mater. Lett. 109 (2013) 31–33. https://doi.org/10.1016/j.matlet.2013.07.039.

[5] K. Krishnaswamy, H. Vali, V. Orsat, Value-adding to grape waste: green synthesis of gold nanoparticles, J. Food Eng. 142 (2014) 210–220. https://doi.org/10.1016/j.jfoodeng.2014.06.014.

[6] A. Slavov, I. Panchev, D. Kovacheva, I. Vasileva, Physico-chemical characterization of water-soluble pectic extracts from *Rosa damascena, Calendula officinalis* and *Matricaria chamomilla* wastes, Food Hydrocolloids 61 (2016) 469–476. https://doi.org/10.1016/j.foodhyd.2016.06.006.

[7] A. Slavov, P. Denev, I. Panchev, V. Shikov, N. Nenov, N. Yantcheva, I. Vasileva, Combined recovery of polysaccharides and polyphenols from *Rosa damascena* wastes, Ind. Crops Prod. 100 (2017) 85–94. https://doi.org/10.1016/j.indcrop.2017.02.017.

[8] A. Slavov, I. Vasileva, L. Stefanov, A. Stoyanova, Valorization of wastes from the rose oil industry, Rev. Environ. Sci. Biotechnol. 16 (2017) 309–325. https://doi.org/10.1007/s11157-017-9430-5.

[9] X. Luo, A. Morrin, A. Killard, M. Smyth, Application of nanoparticles in electrochemical sensors and biosensors, Electroanalysis 18 (2006) 319–326. https://doi.org/10.1002/elan.200503415.

[10] J.M. Pingarrón, P. Yáñez-Sedeño, A. González-Cortés, Gold nanoparticle-based electrochemical biosensors, Electrochim. Acta 53 (2008) 5848–5866. https://doi.org/10.1016/j.electacta.2008.03.005.

[11] F.W. Campbell, S.R. Belding, R. Baron, L. Xiao, R.G. Compton, Hydrogen peroxide electroreduction at a silver-nanoparticle array: investigating nanoparticle size and coverage effects, J. Phys. Chem. C 113 (2009) 9053–9062. https://pubs.acs.org/doi/10.1021/jp900233z.

[12] S. Chen, R. Yuan, Y. Chai, F. Hu, Electrochemical sensing of hydrogen peroxide using metal nanoparticles: a review, Microchim. Acta. 180 (2013) 15–32. https://doi.org/10.1007/s00604-012-0904-4.

[13] G. Doria, J. Conde, B. Veigas, L. Giestas, C. Almeida, M. Assunção, J. Rosa, P. V. Baptista, Noble metal nanoparticles for biosensing applications, Sensors 12 (2012) 1657–1687. https://doi.org/10.3390/s120201657.

[14] A. Hayat, G. Catanante, J.L. Marty, Current trends in nanomaterial-based amperometric biosensors, Sensors 14 (2014) 23439–23461. https://doi.org/10.3390/s141223439.

[15] A.S. Rad, A. Mirabi, E. Binaian, H. Tayebi, A review on glucose and hydrogen peroxide biosensor based on modified electrode included silver nanoparticles, Int. J. Electrochem. Sci. 6 (2011) 3671–3683.

[16] E. Horozova, T. Dodevska, N. Dimcheva, R. Mussarlieva, Electrocatalytic reduction of hydrogen peroxide on palladium-gold codeposits on glassy carbon: applications to the design of interference-free glucose biosensor, Int. J. Electrochem. 2011 (2011) 1–8. Article ID 697698, 8 pages, https://doi.org/10.4061/2011/697698.

[17] A. Longares-Patrón, M.P. Cañizares-Macías, Focused microwaves-assisted extraction and simultaneous spectrophotometric determination of vanillin and p-hydroxybenzaldehyde from vanilla fragans, Talanta 69 (2006) 882–887. https://doi.org/10.1016/j.talanta.2005.11.030.

[18] M. Ohashi, H. Omae, M. Hashida, Y. Sowa, S. Imai, Determination of vanillin and related flavor compounds in cocoa drink by capillary electrophoresis, J. Chromatogr. A 1138 (2007) 262–267. https://doi.org/10.1016/j.chroma.2006.10.031.

[19] K.N. Waliszewski, V.T. Pardio, S.L. Ovando, A simple and rapid HPLC technique for vanillin determination in alcohol extract, Food Chem. 101 (2006) 1059–1062. https://doi.org/10.1016/j.foodchem.2006.03.004.

[20] F. Bettazzi, I. Palchetti, S. Sisalli, M. Mascini, A disposable electrochemical sensor for vanillin detection, Anal. Chim. Acta 555 (2006) 134–138. https://doi.org/10.1016/j.aca.2005.08.069.
[21] P.H. Deng, Z.F. Xu, R.Y. Zeng, C.X. Ding, Electrochemical behavior and voltammetric determination of vanillin based on an acetylene black paste electrode modified with graphene–polyvinylpyrrolidone composite film, Food Chem. 180 (2015) 156–163. https://doi.org/10.1016/j.foodchem.2015.02.035.
[22] L.H. Huang, K.Y. Hou, X. Jia, H.B. Pan, M. Du, Preparation of novel silvernanoplates/graphene composite and their application in vanillin electrochemical detection, Mater. Sci. Eng. C 38 (2014) 39–45. https://doi.org/10.1016/j.msec.2014.01.037.
[23] J. Ning, Q. He, X. Luo, M. Wang, D. Liu, J. Wang, J. Liu, G. Li, Rapid and sensitive determination of vanillin based on a glassy carbon electrode modified with Cu_2O-electrochemically reduced graphene oxide nanocomposite film, Sensors 18 (2018) 2762. https://doi.org/10.3390/s18092762.
[24] P.P.N.V. Kumar, S.V.N. Pammi, P. Kollu, K.V.V. Satyanarayana, U. Shameem, Green synthesis and characterization of silver nanoparticles using *Boerhaavia diffusa* plant extract and their anti-bacterial activity, Ind. Crops Prod. 52 (2014) 562–566. https://doi.org/10.1016/j.indcrop.2013.10.050.
[25] S.M. Roopan, Rohit, G. Madhumitha, A.A. Rahuman, C. Kamaraj, A. Bharathi, T. V. Surendra, Low-cost and eco-friendly phyto-synthesis of silver nanoparticles using *Cocos nucifera* coir extract and its larvicidal activity, Ind. Crops Prod. 43 (2013) 631–635. https://doi.org/10.1016/j.indcrop.2012.08.013.
[26] G.G. Selvam, K. Sivakumar, Phycosynthesis of silver nanoparticles and photocatalytic degradation of methyl orange dye using silver (Ag) nanoparticles synthesized from *Hypnea musciformis* (Wulfen) J.V. Lamouroux,, Appl. Nanosci. 5 (2015) 617–622. https://doi.org/10.1007/s13204-014-0356-8.
[27] S.M. Ghoreishi, M. Behpour, M. Khayatkashani, Green synthesis of silver and gold nanoparticles using *Rosa damascena* and its primary application in electrochemistry, Physica E 44 (2011) 97–104. https://doi.org/10.1016/j.physe.2011.07.008.
[28] M. Lever, A new reaction for colorimetric determination of carbohydrates, Anal. Biochem. 47 (1972) 273–279. https://doi.org/10.1016/0003-2697(72)90301-6.
[29] N. Blumenkrantz, G. Asboe-Hansen, New method for quantitative determination of uronic acids, Anal. Biochem. 54 (1973) 484–489. https://doi.org/10.1016/0003-2697(73)90377-1.
[30] M. DuBois, K. Gilles, J. Hamilton, P. Rebers, F. Smith, Colorimetric method for determination of sugars and related substances, Anal. Chem. 28 (1956) 350–356. https://doi.org/10.1021/ac60111a017.
[31] M.M. Bradford, A rapid and sensitive method for the quantitation of microgram quantities of protein utilizing the principle of protein-dye binding, Anal. Biochem. 72 (1976) 248–254. https://doi.org/10.1016/0003-2697(76)90527-3.
[32] I. Vasileva, R. Denkova, R. Chochkov, D. Teneva, Z. Denkova, T. Dessev, P. Denev, A. Slavov, Effect of lavender (*Lavandula angustifolia*) and melissa (*Melissa Officinalis*) waste on quality and shelf life of bread, Food Chem. 253 (2018) 13–21. https://doi.org/10.1016/j.foodchem.2018.01.131.
[33] W.S. Rasband, U.S. ImageJ, National Institutes of Health, Bethesda, Maryland, USA, 2012. http://imagej.nih.gov/ij/.
[34] J. Puišo, D. Jonkuvienė, I. Mačionienė, J. Šalomskienė, I. Jasutienė, R. Kondrotas, Biosynthesis of silver nanoparticles using lingonberry and cranberry juices and their antimicrobial activity, Colloids Surf., B 121 (2014) 214–221. https://doi.org/10.1016/j.colsurfb.2014.05.001.
[35] P.R. Ghosh, D. Fawcett, S.B. Sharma, G.E.J. Poinern, Production of high-value nanoparticles via biogenic processes using aquacultural and horticultural hood waste, Materials 10 (2017) 852. https://doi.org/10.3390/ma10080852.
[36] L. Castro, M.L. Blázquez, F. González, J.A. Muñoz, A. Ballester, Extracellular biosynthesis of gold nanoparticles using sugar beet pulp, Chem. Eng. J. 164 (2010) 92–97. https://doi.org/10.1016/j.cej.2010.08.034.
[37] R.S. Phatak, A.S. Hendre, Sunlight induced green synthesis of silver nanoparticles using sundried leaves extract of *Kalanchoe pinnata* and evaluation of its photocatalytic potential, Der Pharm. Lett. 7 (2015) 313–324.
[38] E. Turunc, R. Binzet, I. Gumus, G. Binzet, H. Arslan, Green synthesis of silver and palladium nanoparticles using *Lithodora hispidula* (Sm.) Griseb. (Boraginaceae) and application to the electrocatalytic reduction of hydrogen peroxide, Mater. Chem. Phys. 202 (2017) 310–319. https://doi.org/10.1016/j.matchemphys.2017.09.032.
[39] S.F. Adil, M.E. Assal, M. Khan, A. Al-Warthan, M.R.H. Siddiquia, L.M. Liz-Marzán, Biogenic synthesis of metallic nanoparticles and prospects toward green chemistry, Dalton Trans. 44 (2015) 9709–9717. https://doi.org/10.1039/c4dt03222e.
[40] R. Parameshwaran, S. Kalaiselvam, R. Jayavel, Green synthesis of silver nanoparticles using *Beta vulgaris*: role of process conditions on size distribution and surface structure, Mater. Chem. Phys. 140 (2013) 135–147. https://doi.org/10.1016/j.matchemphys.2013.03.012.
[41] R.J.B. Pinto, J.M.F. Lucas, M.P. Morais, S.A.O. Santos, A.J.D. Silvestre, P.A.A. P. Marques, C.S.R. Freire, Demystifying the morphology and size control on the biosynthesis of gold nanoparticles using *Eucalyptus globulus* bark extract, Ind. Crops Prod. 105 (2017) 83–92. https://doi.org/10.1016/j.indcrop.2017.05.003.
[42] P. Velusamy, J. Das, R. Pachaiappan, B. Vaseeharan, K. Pandian, Greener approach for synthesis of antibacterial silver nanoparticles using aqueous solution of neem gum (*Azadirachta indica* L.), Ind. Crops Prod. 66 (2015) 103–109. https://doi.org/10.1016/j.indcrop.2014.12.042.
[43] S. Zhang, Q. Sheng, J. Zheng, Synthesis of Ag-HNTs-MnO_2 nanocomposites and their application for nonenzymatic hydrogen peroxide electrochemical sensing, RSC Adv. 5 (2015) 26878–26885. https://doi.org/10.1039/c5ra01390a.
[44] B. Zhao, Z. Liu, Z. Liu, G. Liu, Z. Li, J. Wang, X. Dong, Silver microspheres for application as hydrogen peroxide sensor, Electrochem. Commun. 11 (2009) 1707–1710. https://doi.org/10.1016/j.elecom.2009.06.035.
[45] W. Hsiao, H. Chen, T. Cheng, T. Huang, Y. Chen, C. Lee, H. Chi, Urchin-like Ag nanowires as non-enzymatic hydrogen peroxide sensor, J. Chin. Chem. Soc. 59 (2012) 500–506. https://doi.org/10.1002/jccs.201100500.
[46] C.Y. Lin, Y.H. Lai, A. Balamurugan, R. Vittal, C.W. Lin, K.C. Ho, Electrode modified with a composite film of ZnO nanorods and Ag nanoparticles as a sensor for hydrogen peroxide, Talanta 82 (2010) 340–347. https://doi.org/10.1016/j.talanta.2010.04.047.
[47] Z. Yang, X. Zheng, J. Zheng, Non-enzymatic sensor based on a glassy carbon electrode modified with Ag nanoparticles/polyaniline/halloysite nanotube nanocomposites for hydrogen peroxide sensing, RSC Adv. 6 (2016) 58329–58335. https://doi.org/10.1039/c6ra06366g.
[48] X. Qin, H. Wang, X. Wang, Z. Miao, Y. Fang, Q. Chen, X. Shao, Synthesis of dendritic silver nanostructures and their application in hydrogen peroxide electroreduction, Electrochim. Acta 56 (2011) 3170–3174. https://doi.org/10.1016/j.electacta.2011.01.058.
[49] L. Zhong, S. Gan, X. Fu, F. Li, D. Han, L. Guo, L. Niu, Electrochemically controlled growth of silver nanocrystals on graphene thin film and applications for efficient nonenzymatic H_2O_2 biosensor, Electrochim. Acta 89 (2013) 222–228. https://doi.org/10.1016/j.electacta.2012.10.161.
[50] M.R. Guascito, E. Filippo, C. Malitesta, D. Manno, A. Serra, A. Turco, A new amperometric nanostructured sensor for the analytical determination of hydrogen peroxide, Biosens. Bioelectron. 24 (2008) 1057–1063. https://doi.org/10.1016/j.bios.2008.07.048.
[51] V. Halouzka, P. Jakubec, C. Gregor, D. Jancik, K. Papadopoulos, T. Triantis, J. Hrbac, Silver-Nafion coated cylindrical carbon fiber microelectrode for amperometric monitoring of hydrogen peroxide heterogeneous catalytic decomposition, Chem. Eng. J. 165 (2010) 813–818. https://doi.org/10.1016/j.cej.2010.10.023.